Research Article Vol. 29, No. 21 / 11 Oct 2021 / Optics Express 32892

Optics EXPRESS

Nonlinear laser-induced frequency shift in a ^{23}Na spin-1 condensate

NINGXUAN ZHENG,[1] WENLIANG LIU,[1,2,4] VLADIMIR SOVKOV,[1,3] JING XU,[1] GUIYUAN GE,[1] YUQING LI,[1,2] PENG LI,[1] YONGMING FU,[1] JIZHOU WU,[1,2,5] JIE MA,[1,2,6] LIANTUAN XIAO,[1,2] AND SUOTANG JIA[1,2]

[1] *State Key Laboratory of Quantum Optics and Quantum Optics Devices, Institute of Laser Spectroscopy, Shanxi University, Taiyuan 030006, China*
[2] *Collaborative Innovation Center of Extreme Optics, Shanxi University, Taiyuan 030006, China*
[3] *St. Petersburg State University, 7/9 Universitetskaya nab., St. Petersburg 199034, Russia*
[4] *liuwl@sxu.edu.cn*
[5] *wujz@sxu.edu.cn*
[6] *mj@sxu.edu.cn*

Abstract: Herein, we report on the experimental observations and a quantitative determination of the laser-induced frequency shift (LIFS) in the photoassociation (PA) spectra of spinor Bose-Einstein condensate of sodium. Our investigations revealed a nonlinear dependence of the LIFS on the intensity of PA laser. By developing a model within the quadratic Stark effect, we simulate the experimental results via a theoretical model that confirms the former. The experimental observations and the theoretical analysis can further improve the accuracy of investigations on important molecular properties and on preparation of specific molecular states, with possible applications in various key fields.

1. Introduction

Bose-Einstein condensates (BECs) of atomic gases are ideal platforms for observing versatile microscopic quantum effects [1,2]. An important approach in investigating quantum gas is by forming the ultracold quantum gas of molecules [3–6]. Photoassociation (PA) of atoms in a BEC has been established as a standard method for the production of ultracold molecules [7]. The fabrication and manipulation of ultracold molecules have been intensively studied recently, as the latter are expected to have relevant applications in fields like precision measurement or quantum information processing [8].

The laser-induced frequency shift (LIFS) has always been considered an important phenomenon during the PA process. The LIFS corresponding to a specific ro-vibrational level in the ultracold molecules stems from the energy coupling between the atomic scattering state (or free state) and the molecular bound state during a PA transitional process. It has a key role in the preparation of ultracold molecules in specific states [9] and manipulation of ultracold molecular quantum states [10]. While investigating the LIFS, it is beneficial to employ PA to change the interactions between ultracold atoms [11–14]. The LIFS linear relation coefficient of laser intensity has served as a versatile tool for measuring the s-wave scattering length [15], investigating anomalous quantum correlations [16] and manipulating individual hyperfine states in ultracold molecular ions [17].

LIFS has been reported to occur in ultracold alkali molecular samples of Li_2 [13,18], Na_2 [19], Rb_2 [20], Cs_2 [21], and the heteronuclear molecule NaCs [22]. It has been successfully controlled via an external magnetic field in ultracold Cs_2 molecules formed by PA [23]. Moreover, various possibilities to eliminate the light shift of the atoms in the optical tweezers have been investigated

#437881 https://doi.org/10.1364/OE.437881
Journal © 2021 Received 15 Jul 2021; revised 26 Aug 2021; accepted 13 Sep 2021; published 27 Sep 2021

Optics EXPRESS

[24]. Altogether, these studies, both theoretical predictions and experimental measurements, demonstrate a linear dependence between the shift and intensity of the PA laser.

In this study, we carried out a systematic experimental study on the influence of PA laser and ^{23}Na spinor condensate during the production of Na_2 molecules. A nonlinear LIFS is observed and measured. We present a theoretical analysis for explaining the nonlinearity of this LIFS via the quadratic Stark effect, which is confirmed by experimental results. Our study reveals that the observed nonlinear shift can contribute to further improving the accuracy of investigations of important molecular properties and preparation of specific molecular states. Moreover, the nonlinear effect opens the gate toward investigating the effect of high-order AC Stark effect on the atoms [25]. Furthermore, the experimentally measured coefficients of the first-order and second-order terms provide an opportunity for predicting and analyzing the Stark effect under high AC field strengths.

2. Experiments

The Na spinor condensates are prepared via a typical optical approach, following [26]. The experimental system consists of three parts: oven cavity, intermediate cavity, and science chamber. The solid sodium is heated to generate an atom beam in the oven cavity. The intermediate cavity is a Zeeman slower to decelerate the atoms ejected from the oven cavity. The schema of the science chamber is shown in Fig. 1. The atoms are collected in the MOT after the initial deceleration by the Zeeman slower. Compressed MOT and optical molasses are implemented afterwards by increasing the laser power and the frequency detuning while decreasing the magnetic field gradient. To cool the atomic cloud to condensation, a crossed optical dipole trap (CODT), created by two large-detuned laser beams along the axes sketched in Fig. 1, is applied with the aim of loading and evaporatively cooling the atoms. After the free evaporation (0.5 s) and the forced evaporation (3 s), a BEC of $\sim 3 \times 10^5$ ^{23}Na atoms in the $F = 1$ state with a temperature of ~ 50 nK is produced. The trap frequencies of the CODT are $(\omega_x, \omega_y, \omega_z) = 2\pi \times (325, 321, 385$ Hz), leading to a condensated dimension of 21 μm and a phase space density of 8.2.

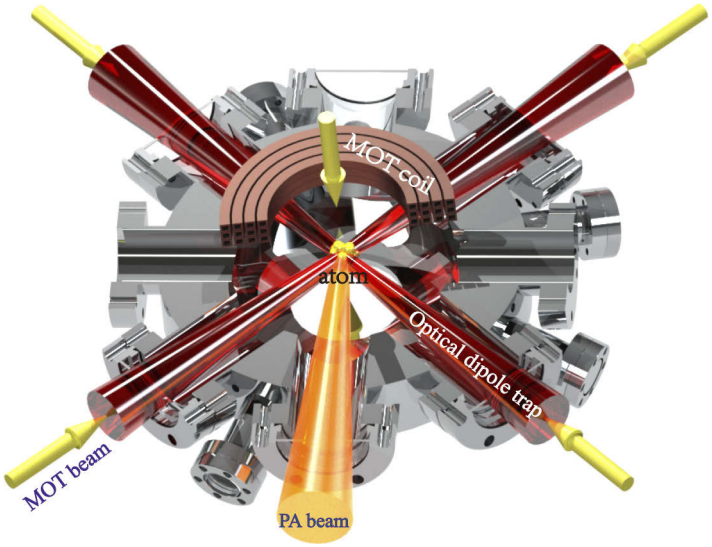

Fig. 1. The experimental device of the science chamber. The magneto-optical trap (MOT) beams are represented by yellow arrows. The spinor BEC (yellow balls) are prepared in a crossed optical dipole trap (red beams). A PA beam (orange beam) is focused on the spinor BEC.

Optics EXPRESS

The PA is induced by an additional frequency-doubled tunable diode laser system (Toptica, TA-SHG) with a wavelength of 589 nm, linewidth of 0.1 MHz, and an output power of 1.1 W. The frequency of the PA laser is tuned to near resonance with the $v = 4$ vibrational level of the pure long-range 0_g^- state (corresponding to a wavenumber of 16972.438 cm^{-1}) below the Na_2 $3S_{1/2} + 3P_{3/2}$ dissociation limit. There is no other PA spectrum in the vicinity of 300 MHz near this level, which is a good choice for studying the LIFS. The absolute PA laser frequency is measured and locked by a high-precision wavelength meter (HighFinesse WSU), which is calibrated against the Na atomic hyperfine resonance transition ($|F = 2\rangle \rightarrow |F' = 3\rangle$) at the beginning of each experimenting cycle. The measured frequency accuracy is ~ 5 MHz [22].

The PA beam waist focuses on the spinor BEC with a full length at half maximum of 108 μm. The radius of the waist depends on the size of the BEC and a small waist allows the intensity to have a larger range to regulate. The intensity can be controlled from 16 to 2880 W·cm^{-2}. The position of the beam has been calibrated many times to confirm that the PA laser beam fully interacts with the atoms. The PA laser duration under different power densities determined by a fixed parameter (intensity × duration) is optimized between 18000 and 100 μs ensuring that the spectrum at each intensity is close to saturation and the fitting of resonance position is accurate.

The experimental spectra measured with different pulse durations under the same intensity are presented in Fig. 2(a), whereas Fig. 2(b) shows the corresponding saturation phenomenon of atomic loss. The PA resonance can be detected when the excited state molecule formed by the PA laser spontaneously decays into the ground-state molecule or becomes a hot atom pair escaping the trap. According to the results depicted in Fig. 2, the suitable parameter in our experiment is set to be 288 ms·W·cm^{-2} (the consideration for not choosing a larger parameter here is to maintain a longer duration under a high power of PA). Changing of the duration would not cause a shift of the PA resonance frequency. The switch of the PA laser is controlled by a fast-response acousto-optical modulator (Gooch & Housego 3080-125), whose rise time is as short as 60 ns. An external bias magnetic field of about 100 mG is applied along the direction of gravity, which is defined as the magnetic quantization axis. The polarization of the PA laser is linear and parallel with the magnetic quantization axis.

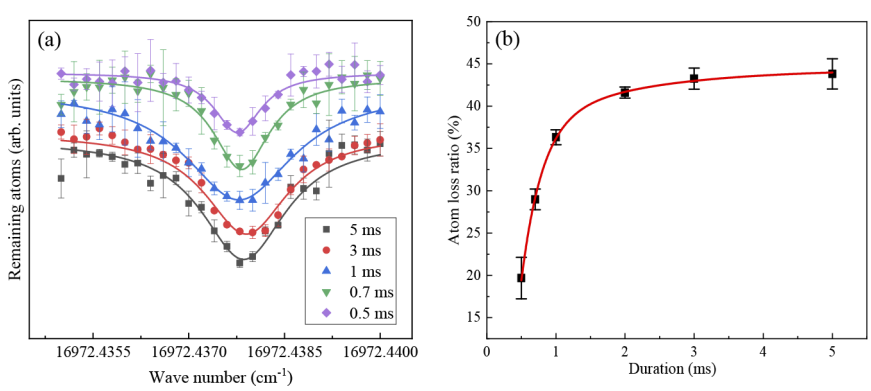

Fig. 2. (a) The PA spectra for different durations of the PA pulse under the intensity of 226 W·cm^{-2}. The resonance locations of the PA peaks are determined by fitting the data with Lorentzian curves (represented by solid curves). There is no statistically significant correlation between the resonance location and PA duration. (b) Saturation of atomic loss ratio at the intensity of 226 W·cm^{-2}.

Figure 3 shows a series of typical trap loss PA spectra induced by different intensities of the PA laser. The interval of each considered data point was 6 MHz and the corresponding points were measured thrice. The number of atoms remaining in the trap after the action of PA laser was determined by the absorption images with 5 ms time-of-flight. The final values were

Optics EXPRESS

obtained by averaging and normalizing the number of atoms measured during three experiments. The resonance locations of the PA peaks were determined by fitting the data to corresponding Lorentzian curves. Figure 3 clearly shows the shift of the resonance position in the PA spectrum induced by increasing the PA laser intensity.

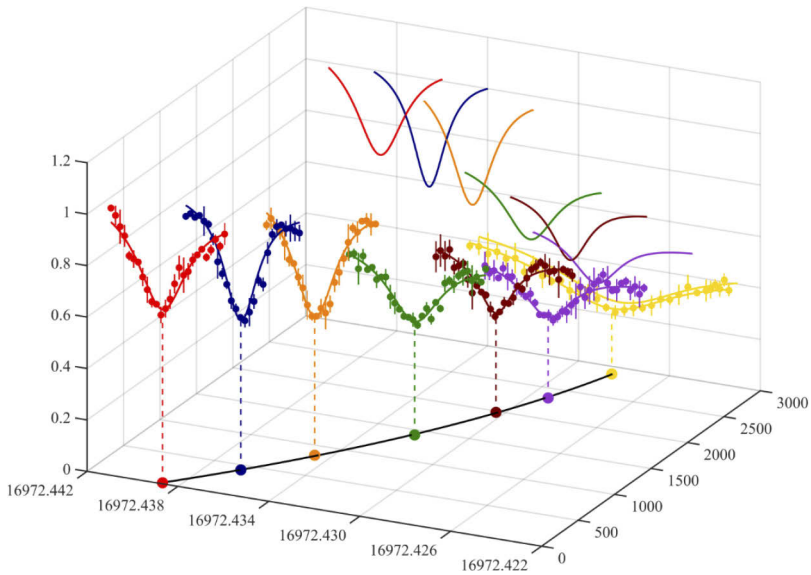

Fig. 3. The PA spectra of the $v = 4$ molecular vibrational level of the Na_2 0_g^- pure long-range state for seven different PA laser intensities: I_{PA} = 16.2 W·cm^{-2} (red), 420 W·cm^{-2} (blue), 840 W·cm^{-2} (orange), 1416 W·cm^{-2} (green), 1980 W·cm^{-2} (brown), 2340 W·cm^{-2} (purple) and 2880 W·cm^{-2} (yellow). The resonance locations of the PA peaks were determined by fitting the data with corresponding Lorentzian curves (solid curves). The curves on the rear panels are the projection of the fitted curves. The resonance positions are projected on the bottom surface and fitted with quadratic functions.

3. Results and analysis

In Fig. 4, both the PA resonance positions and PA laser intensities are shown. Below the intensity of 1.5 kW·cm^{-2}, the observed linear dependence of the spectral shift on the laser intensity is consistent with the calculation based on the multichannel scattering theory [12,13] and the measured LIFS slope is −141.62 ± 5.54 MHz/(kW·cm^{-2}). However, when the power is increased to 2.8 kW·cm^{-2}, the nonlinear dependence of the spectral shift on the laser intensity can be clearly noticed. The fit of this dependence with the quadratic function (−166.09 (± 3.47) I_{PA} + 18.76 (± 1.40) I_{PA}^2 + 1.38 (± 1.72)) MHz is also shown in Fig. 4. The first-order and second-order coefficients are −166.09 (± 3.47) MHz/(kW·cm^{-2}) and 18.76 (± 1.40) MHz/(kW·cm^{-2})^2 respectively.

In our recent study [27] on the magnetically manipulated PA LIFS in ultracold caesium, we adopted a three-channel model within the method of Green functions [28,29]. The three channels are (1) the continuum of states P, (2) single neighboring level Q, and (3) excited light-dressed photoassociated level R. The energies of these unperturbed (neglecting couplings) states are E, ϵ_Q, and ϵ_R. In our simplified theory, we neglected the thermal average and considered a fixed (already averaged) scattering energy: the spread of the real thermal energies is expected to be very narrow in a BEC. Here we employed the same model with all the equations rederived by using the projection technique by Feshbach [30–32].

Optics EXPRESS

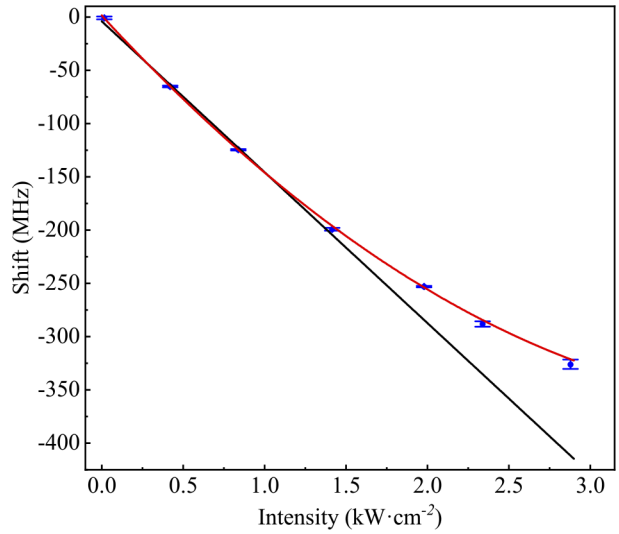

Fig. 4. The spectral shift as a function of the PA laser intensity for the $v = 4$ molecular vibrational level of the Na_2 long-range 0_g^- state for the spinor BEC. The black solid line is the linear fit of the initial fragment (< 1.5 kW·cm^{-2}) and the red solid curve is the quadratic fit of the full-range data.

The resulting expression for the optical transition probability in this system is

$$\rho(E,\delta) = \frac{w(E)}{\pi}\frac{1}{(\delta-\delta_m)^2 + w(E)^2}, \tag{1}$$

where δ is the energy shift (the experimental transition energy is $\hbar\omega = \epsilon_R - E + \delta$).

The first factor $w(E)/\pi$ coincides with the famous Fano result [33,34] for the transition probability from the lower coupled state $P \sim Q$ with the energy E to the unperturbed upper state (the weak intensity approximation):

$$\frac{w(E)}{\pi} = |W_{PR}|^2\left[\frac{(\beta+q)^2}{\beta^2+1}\right], \tag{2}$$

where W_{XY} is the coupling matrix element between the channels X and Y,

$$\beta = \frac{E - \epsilon_Q - F_{QQ}}{\pi|W_{PQ}|^2}$$

is the reduced initial energy,

$$q = \frac{W_{RQ} + F_{QR}}{\pi W_{QP} W_{RP}}$$

is the Fano asymmetry parameter,

$$F_{XY}(E) = \mathcal{P}\int \frac{W_{XP}(\epsilon_P)W_{PY}(\epsilon_P)}{E-\epsilon_P}\,d\epsilon_P,$$

and $\mathcal{P}$ denotes the principal value of the integral.

The other (second) factor of Eq. (1), as a function of the shift δ, is the Lorentzian, in agreement with the experimental observations (Figs. 2(a) and 3). The full width at half maximum (FWHM)

Optics EXPRESS

$2w(E)$ is determined by Eq. (2). The position of the maximum is

$$\delta_m = \pi|W_{PR}|^2 \left[\frac{(q^2-1)\beta - 2q}{\beta^2+1}\right] - F_{RR} \equiv \pi|W_{PR}|^2 S - F_{RR} \tag{3}$$

The only PA-intensity dependent quantity in the above equations is the optical coupling matrix element (transition amplitude) W_{PR}, which is a linear function of the electric field $\mathcal{E} \sim \sqrt{I_{PA}}$. Hence, within the considered model, (see Eqs. (2), 3) both the peak position δ_m and its FWHM are linear functions of the PA laser intensity I_{PA}. The parameters of the profile Eqs. (2) and 3 depend on the energy ϵ_Q of the near-dissociation bound level, i.e., implicitly on the scattering length (e. g., [35]).

The model described above is obviously oversimplified. Its success in explaining a bulk of experimental observations (e. g., Ref. [27]) proves that it successfully captures the principal mechanisms of the laser-induced shifts in PA. Nonetheless, there are different effects not taken into account by it, which are useful for improving its predictions. These effects include a possible influence of other bound or scattering channels besides the already considered three, multiparticle interactions in the condensate, or high-order Stark effects. The easiest way to correct our model phenomenologically is by including the quadratic Stark effect with a supposition that it is able to effectively incorporate all other effects. This would be able to produce a nonlinear dependence of the shift δ_m on the PA laser intensity I_{PA}.

For the sake of simplicity, let us restrict ourselves to the diagonal quadratic ($\sim \mathcal{E}^2$ with the electric field $\mathcal{E} \sim \pm\sqrt{I}$) Stark effect with the Hamiltonian matrix element

$$\langle Q\,|\mathbf{H}|\,Q\rangle \approx \epsilon_Q + \epsilon'_Q I. \tag{4}$$

Provided this dependence is weak, the relation

$$\frac{\epsilon'_Q}{\epsilon_Q} I \ll 1 \tag{5}$$

holds all the way. Let us approximate Eq. (3) within a first order of this ratio. This gives for the reduced energy

$$\beta = \frac{E - (\epsilon_Q + \epsilon'_Q I) - F_{QQ}}{\pi|W_{PQ}|^2} \equiv \beta_0 + \beta'_0 I$$

with β_0 coinciding with β by neglecting the quadratic Stark effect and

$$\beta'_0 = -\frac{\epsilon'_Q}{\pi|W_{PQ}|^2}.$$

Then, for the profile function one has

$$S = \frac{(q^2-1)(\beta_0 + \beta'_0 I) - 2q}{(\beta_0 + \beta'_0 I)^2 + 1} \approx S_0 + S'_0 I$$

with S_0 coinciding with S by neglecting the quadratic Stark effect and

$$S'_0 = -2S_0 \frac{\beta_0 \beta'_0}{\beta_0^2+1} = \frac{2S_0}{\pi|W_{PQ}|^2} \frac{\beta_0}{\beta_0^2+1} \epsilon'_Q.$$

Finally,

$$\delta_m \approx \left[\pi|w_{PR}|^2 S_0 - f_{RR}\right] I_{PA} + 2S_0 \left|\frac{w_{PR}}{W_{PQ}}\right|^2 \frac{\beta_0 \epsilon'_Q}{\beta_0^2+1} I_{PA}^2 \tag{6}$$

with the lower-case designations for the same values as the upper-case ones, but relating the unit intensity $I_{PA} = 1$.

Optics EXPRESS

Without an external magnetic field (or with a weak enough field), the bound level lies below the threshold, whereas the scattering state lies above it, so it is expected that $\beta_0>0$. It is known that for the ground state atoms the quadratic Stark effect is negative, so it is expected that for the near-dissociation molecular levels one has $\epsilon'_Q<0$. Hence, the coefficient of I^2 is expected to have the opposite sign to the one of S_0. In our case, we observed that $S_0<0$, which makes the quadratic coefficient positive, in accordance with the experimental observations.

4. Conclusions

We identified a nonlinear dependence of LIFS and PA laser intensity and noted that at a comparably high intensity the influence of the quadratic Stark effect, it is actually not negligible. To describe this phenomenon, we propose a simple phenomenological theory, which provides a theoretical basis for LIFS at a high power, thereby improving the existing theories. The first-order and second-order coefficients determined in the experiment can further improve the subsequent predictions and analysis of the Stark effect under high AC field strengths. Thus, our new findings have the potential to pave the way for a series of significant preparations and manipulations of ultracold molecules, with possible applications in various key fields.

Funding. National Key Research and Development Program of China (2017YFA0304203); National Natural Science Foundation of China (62011530047, 61901249, 62020106014); PCSIRT (IRT-17R70); 111 Project (D18001); Program for the Outstanding Innovative Teams of Higher Learning Institutions of Shanxi (OIT); the Applied Basic Research Project of Shanxi Province, China (201901D211188, 201901D211191); the Shanxi 1331 KSC (the Shanxi 1331 KSC); Russian Foundation for Basic Research20-53-53025

Disclosures. The authors declare no conflicts of interest.

Data availability. Data underlying the results presented in this paper are not publicly available at this time but may be obtained from the authors upon reasonable request.

References

1. M. H. Anderson, J. R. Ensher, M. R. Matthews, C. E. Wieman, and E. A. Cornell, "Observation of Bose-Einstein condensation in a dilute atomic vapor," Science **269**(5221), 198–201 (1995).
2. K. B. Davis, M. O. Mewes, M. R. Andrews, N. J. van Druten, D. S. Durfee, D. M. Kurn, and W. Ketterle, "Bose-Einstein condensation in a gas of sodium atoms," Phys. Rev. Lett. **75**(22), 3969–3973 (1995).
3. Z. Zhang, L. Chen, K.-X. Yao, and C. Chin, "Transition from an atomic to a molecular Bose-Einstein condensate," Nature **592**(7856), 708–711 (2021).
4. P. K. Molony, P. D. Gregory, Z. Ji, B. Lu, M. P. Köppinger, C. R. Le Sueur, C. L. Blackley, J. M. Hutson, and S. L. Cornish, "Creation of ultracold ^{8}7Rb^{1}33Cs molecules in the rovibrational ground state," Phys. Rev. Lett. **113**(25), 255301 (2014).
5. J. W. Park, S. A. Will, and M. W. Zwierlein, "Ultracold dipolar gas of fermionic ^{2}3Na^{4}0K molecules in their absolute ground state," Phys. Rev. Lett. **114**(20), 205302 (2015).
6. M. Guo, B. Zhu, B. Lu, X. Ye, F. Wang, R. Vexiau, N. Bouloufa-Maafa, G. Quéméner, O. Dulieu, and D. Wang, "Creation of an ultracold gas of ground-state dipolar ^{2}3Na^{8}7Rb molecules," Phys. Rev. Lett. **116**(20), 205303 (2016).
7. K. M. Jones, E. Tiesinga, P. D. Lett, and P. S. Julienne, "Ultracold photoassociation spectroscopy: Long–range molecules and atomic scattering," Rev. Mod. Phys. **78**(2), 483–535 (2006).
8. L. D. Carr, D. DeMille, R. V. Krems, and J. Ye, "Cold and ultracold molecules: science, technology and applications," New J. Phys. **11**(5), 055049 (2009).
9. J. G. Danzl, M. J. Mark, E. Haller, M. Gustavsson, R. Hart, J. Aldegunde, J. M. Hutson, and H.-C. Nägerl, "An ultracold high-density sample of rovibronic ground-state molecules in an optical lattice," Nat. Phys. **6**(4), 265–270 (2010).
10. S. Ospelkaus, K. K. Ni, D. Wang, M. H. G. de Miranda, B. Neyenhuis, G. Quéméner, P. S. Julienne, J. L. Bohn, D. S. Jin, and J. Ye, "Quantum-state controlled chemical reaction of ultracold potassium-rubidium molecules," Science **327**(5967), 853–857 (2010).
11. P. O. Fedichev, Y. Kagan, G. V. Shlyapnikov, and J. T. M. Walraven, "Influence of nearly resonant light on the scattering length in low-temperature atomic gases," Phys. Rev. Lett. **77**(14), 2913–2916 (1996).
12. J. L. Bohn and P. S. Julienne, "Prospects for influencing scattering lengths with far-off-resonant light," Phys. Rev. A: At., Mol., Opt. Phys. **56**(2), 1486–1491 (1997).
13. J. M. Gerton, B. J. Frew, and R. G. Hulet, "Photoassociative frequency shift in a quantum degenerate gas," Phys. Rev. A: At., Mol., Opt. Phys. **64**(5), 053410 (2001).
14. C. Chin, R. Grimm, P. Julienne, and E. Tiesinga, "Feshbach resonances in ultracold gases," Rev. Mod. Phys. **82**(2), 1225–1286 (2010).

Optics EXPRESS

15. J. Kim, S. Moal, M. Portier, J. Dugué, M. Leduc, and C. Cohen-Tannoudji, "Frequency shifts of photoassociative spectra of ultracold metastable helium atoms: A new measurement of the *s*-wave scattering length," Europhys. Lett. **72**(4), 548–554 (2005).
16. M. Mackie, "Anomalous frequency shift in the photoassociation spectrum of a Bose-Einstein condensate," Phys. Rev. Lett. **91**(17), 173004 (2003).
17. U. Bressel, A. Borodin, J. Shen, M. Hansen, I. Ernsting, and S. Schiller, "Manipulation of individual hyperfine states in cold trapped molecular ions and application to HD^+ frequency metrology," Phys. Rev. Lett. **108**(18), 183003 (2012).
18. I. D. Prodan, M. Pichler, M. Junker, R. G. Hulet, and J. L. Bohn, "Intensity dependence of photoassociation in a quantum degenerate atomic gas," Phys. Rev. Lett. **91**(8), 080402 (2003).
19. C. McKenzie, J. Hecker Denschlag, H. Häffner, A. Browaeys, L. E. E. de Araujo, F. K. Fatemi, K. M. Jones, J. E. Simsarian, D. Cho, A. Simoni, E. Tiesinga, P. S. Julienne, K. Helmerson, P. D. Lett, S. L. Rolston, and W. D. Phillips, "Photoassociation of sodium in a Bose-Einstein condensate," Phys. Rev. Lett. **88**(12), 120403 (2002).
20. A. Simoni, P. S. Julienne, E. Tiesinga, and C. J. Williams, "Intensity effects in ultracold photoassociation line shapes," Phys. Rev. A: At., Mol., Opt. Phys. **66**(6), 063406 (2002).
21. J. Wu, Z. Ji, Y. Zhang, L. Wang, Y. Zhao, J. Ma, L. Xiao, and S. Jia, "High sensitive determination of laser-induced frequency shifts of ultracold cesium molecules," Opt. Lett. **36**(11), 2038–2040 (2011).
22. W. Liu, X. Wang, J. Wu, X. Su, S. Wang, V. B. Sovkov, J. Ma, L. Xiao, and S. Jia, "Experimental observation and determination of the laser-induced frequency shift of hyperfine levels of ultracold polar molecules," Phys. Rev. A: At., Mol., Opt. Phys. **96**(2), 022504 (2017).
23. Y. Li, G. Feng, W. Liu, J. Wu, J. Ma, L. Xiao, and S. Jia, "Control of laser-induced frequency shift in ultracold cesium molecules by an external magnetic field," Opt. Lett. **40**(10), 2241–2244 (2015).
24. N. R. Hutzler, L. R. Liu, Y. Yu, and K.-K. Ni, "Eliminating light shifts for single atom trapping," New J. Phys. **19**(2), 023007 (2017).
25. N. B. Delone and V. P. Krainov, "AC stark shift of atomic energy levels," Phys.-Usp. **42**(7), 669–687 (1999).
26. J. Jiang, L. Zhao, M. Webb, N. Jiang, H. Yang, and Y. Liu, "Simple and efficient all-optical production of spinor condensates," Phys. Rev. A **88**(3), 033620 (2013).
27. Y. Li, X. Wang, J. Wu, G. Feng, W. Liu, V. Sovkov, J. Ma, B. Deb, L. Xiao, and S. Jia, "The effects of a Feshbach resonance on spectral shifts in photoasociation of Cs atoms," Phys. Chem. Chem. Phys. **23**(1), 641–646 (2021).
28. B. Deb and G. S. Agarwal, "Feshbach resonance-induced Fano interference in photoassociation," J. Phys. B: At., Mol. Opt. Phys. **42**(21), 215203 (2009).
29. B. Deb, "Magneto-optical Feshbach resonance: controlling cold collision with quantum interference," J. Phys. B: At., Mol. Opt. Phys. **43**(8), 085208 (2010).
30. H. Feshbach, "Unified theory of nuclear reactions," Ann. Phys. **5**(4), 357–390 (1958).
31. H. Feshbach, "A unified theory of nuclear reactions. II," Ann. Phys. **19**(2), 287–313 (1962).
32. H. Feshbach, "The unified theory of nuclear reactions," Ann. Phys. **43**(3), 410–420 (1967).
33. U. Fano, "Effects of configuration interaction on intensities and phase shifts," Phys. Rev. **124**(6), 1866–1878 (1961).
34. U. Fano and J. W. Cooper, "Line profiles in the far-uv absorption spectra of the rare gases," Phys. Rev. **137**(5A), A1364–A1379 (1965).
35. C. D. Hamley, E. M. Bookjans, G. Behin-Aein, P. Ahmadi, and M. S. Chapman, "Photoassociation spectroscopy of a spin-1 Bose-Einstein condensate," Phys. Rev. A: At., Mol., Opt. Phys. **79**(2), 023401 (2009).